Relativistic random-phase approximation longitudinal response function for quasielastic electron scattering

K. Wehrberger and F. Beck
Institut für Kernphysik, Technische Hochschule Darmstadt, D-6100 Darmstadt, Federal Republic of Germany
(Received 1 October 1987)

The longitudinal response function for quasielastic electron scattering is calculated in the $\sigma\omega\rho$ model of quantum hadrodynamics. We use meson fields and nucleon wave functions, as obtained in mean-field theory of closed-shell nuclei, in relativistic random-phase approximation. The results for ^{12}C and ^{40}Ca are compared with those of a previous calculation, where the response function was evaluated in local-density approximation. We find a shift in the position of the maximum which is due to the inclusion of binding energy effects, and a slight broadening of the response function. Comparing with the data, we find good agreement except for ^{40}Ca at the highest momentum transfer $q = 550$ MeV.

I. INTRODUCTION

Relativistic field theories of nucleons interacting with scalar and vector mesons have attracted general interest in recent years.[1] Quantum hadrodynamics has been successful in explaining the ground-state properties of nuclear matter and nuclei.[2] It is therefore of interest to investigate the implications of this model for dynamical processes like the interaction of nuclei with nucleons and electrons. In this work we study quasielastic electron scattering in the framework of the $\sigma\omega\rho$ model of quantum hadrodynamics.

Measurements of the separated longitudinal and transverse response functions became available some years ago and have since been a challenge to any theory of nuclear structure. In Refs. 3 and 4 the response functions for nuclear matter have been calculated in the $\sigma\omega\rho$ model in relativistic random-phase approximation (RPA). In Ref. 5 we have calculated the response functions for finite nuclei in local-density approximation using these results together with local nucleon densities and meson fields as obtained from the solution of the mean-field equations of this model. The RPA-correlations were found to reduce the longitudinal response function significantly with respect to the Hartree result, but the transverse response function is almost unchanged. We obtained good agreement with the data for both response functions using free nucleon form factors.

While the local-density approximation is, in general, a good approximation in the quasielastic region, it does, e.g., not include the separation energy of the nucleons.[5] In the present work we therefore improve the previous calculation by using the wave functions and binding energies of the nucleons as evaluated in the $\sigma\omega\rho$ model in relativistic random-phase approximation for finite nuclei. We use the same meson masses and coupling constants as in Ref. 5, determined from the ground-state properties of nuclear matter and closed-shell nuclei.[2] As the authors of Ref. 6, who calculate the response of nuclei in the Hartree-approximation, we employ the Green's function method.[7] As noted above, Hartree- and RPA results almost agree with each other in the transverse channel. Therefore, we restrict our calculations with the exact one-body density to the longitudinal response function.

The calculation is fully consistent in the sense that the wave functions of the nucleons and the RPA renormalization are calculated within the same model. This is in contrast to comparable nonrelativistic calculations, where the wave functions are calculated in a harmonic oscillator potential, while some phenomenological parametrization is chosen for the particle-hole interaction.[8,9] Furthermore, by using the Green's function method, the continuum, which is usually neglected,[8] is fully included.

Employing the Green's function technique, the RPA equations for a nontranslational invariant system can be solved by iteration. We check for convergence carefully by comparison with the exactly solvable local-density approach and find satisfactory convergence after the second iteration.

In Sec. II we outline our method to solve the relativistic RPA equations for finite nuclei. Section III contains results for the two experimentally well studied nuclei ^{12}C and ^{40}Ca, in comparison with previous local-density results and the measured response functions. Section IV gives our conclusions.

II. RANDOM-PHASE APPROXIMATION

The longitudinal response function for quasielastic electron scattering with momentum transfer $q = |\mathbf{q}|$ and energy transfer ω is given by[10]

$$S_L(q,\omega) = \frac{1}{\pi}\mathrm{Im}\Pi(j_L,j_L;q,q,\omega) \ . \tag{1}$$

Here j_L is the zero component of the effective baryon current j_μ as given in Ref. 5 which includes the nucleon Dirac and Pauli form factors. The polarization propagator Π is defined by

$$\Pi(A,B;\mathbf{q}_1,\mathbf{q}_2;\omega)=\int d^3x e^{-i\mathbf{q}_1\mathbf{x}}\int d^3y e^{i\mathbf{q}_2\mathbf{y}}\Pi(A(\mathbf{x}),B(\mathbf{y});\omega) \tag{2}$$

with

$$\Pi(A(\mathbf{x}),B(\mathbf{y});\omega)=\sum_n\left[\frac{\langle\Psi_0|A^\dagger(\mathbf{x})|\Psi_n\rangle\langle\Psi_n|B(\mathbf{y})|\Psi_0\rangle}{E_n-E_0-\omega-i\epsilon}+\frac{\langle\Psi_0|B(\mathbf{y})|\Psi_n\rangle\langle\Psi_n|A^\dagger(\mathbf{x})|\Psi_0\rangle}{E_n-E_0+\omega+i\epsilon}\right]. \tag{3}$$

This equation is exact if Ψ_0 and Ψ_n describe the ground state and excited states of the nucleus exactly. In the Hartree approximation the ground state is approximated by the Slater determinant of occupied levels, the excited states by particle-hole pairs. Thus, the interaction of the particle-hole pair which is created by the external field is neglected. In random-phase approximation this interaction is taken into account by summing the ring diagrams to all orders. The corresponding Dyson equation for the polarization propagator $\tilde{\Pi}$ in random-phase approximation in terms of the propagator Π in the Hartree approximation reads in momentum space (argument ω omitted)

$$\tilde{\Pi}(A,B;\mathbf{q},\mathbf{q}')=\Pi(A,B;\mathbf{q},\mathbf{q}')-\sum_{C,D}\int\frac{d^3q''}{(2\pi)^3}\tilde{\Pi}(A,C;\mathbf{q},\mathbf{q}'')V_{C,D}(\mathbf{q}'')\Pi(D,B;\mathbf{q}'',\mathbf{q}'), \tag{4}$$

where V stands for the interaction, i.e., exchange of σ, ω, and ρ mesons. In nuclear matter this equation reduces to the RPA matrix equation as given in Ref. 3 because of translational invariance.

The effective current component j_0 has two parts; the Dirac current and the anomalous current. For the momentum and energy transfers considered here ($\omega\leq q\leq 550$ MeV) the Dirac current gives the dominant contribution to the total longitudinal response function, while the anomalous current contributes less than 25%. Therefore, we calculate the RPA corrections only for the Dirac current and treat the contribution from the anomalous current in the Hartree approximation. This reduces the number of integral equations considerably. The nucleon wave functions are evaluated in the $\sigma\omega\rho$ model which includes the Coulomb interaction. In evaluating the longitudinal response, however, we reduce the numerical effort further by using the proton wave functions also for the neutrons. This is a good approximation for the symmetric nuclei considered (^{12}C and ^{40}Ca), especially since the neutrons contribute only a little to the longitudinal response.

With Eq. (1), the Dirac contribution $S_{L,D}$ to the longitudinal response function in random-phase approximation reads

$$S_{L,D}(q,\omega)=\frac{1}{\pi}\mathrm{Im}\tilde{\Pi}(\gamma_0\tau_p,\gamma_0\tau_p;q,q;\omega) \qquad [\tau_p=\tfrac{1}{2}(1+\tau_3)]. \tag{5}$$

(Here and in the following equations the nucleon form factors are, in order to simplify the notation, not denoted explicitly.) For the evaluation of $\tilde{\Pi}$, the following system of integral equations has to be solved:

$$\begin{aligned}\tilde{\Pi}(\gamma_\alpha\tau_p,\gamma_\beta\tau_p;\mathbf{q},\mathbf{q}')=&\Pi(\gamma_\alpha\tau_p,\gamma_\beta\tau_p;\mathbf{q},\mathbf{q}')+\int\frac{d^3q''}{(2\pi)^3}\tilde{\Pi}(\gamma_\alpha\tau_p,1;\mathbf{q},\mathbf{q}'')\chi_s(q'')\Pi(1,\gamma_\beta\tau_p;\mathbf{q}'',\mathbf{q}')\\&-\int\frac{d^3q''}{(2\pi)^3}\tilde{\Pi}(\gamma_\alpha\tau_p,\gamma_\mu 1;\mathbf{q},\mathbf{q}'')\chi_V(q'')\Pi(\gamma^\mu 1,\gamma_\beta\tau_p;\mathbf{q}'',\mathbf{q}')\\&-\sum_{i=1}^{3}\int\frac{d^3q''}{(2\pi)^3}\tilde{\Pi}(\gamma_\alpha\tau_p,\gamma_\mu\tau_i;\mathbf{q},\mathbf{q}'')\chi_\rho(q'')\Pi(\gamma^\mu\tau_i,\gamma_\beta\tau_p;\mathbf{q}'',\mathbf{q}'),\end{aligned} \tag{6}$$

$$\begin{aligned}\tilde{\Pi}(\gamma_\alpha\tau_p,1;\mathbf{q},\mathbf{q}')=&\Pi(\gamma_\alpha\tau_p,1;\mathbf{q},\mathbf{q}')+\int\frac{d^3q''}{(2\pi)^3}\tilde{\Pi}(\gamma_\alpha\tau_p,1;\mathbf{q},\mathbf{q}'')\chi_s(q'')\Pi(1,1;\mathbf{q}'',\mathbf{q}')\\&-\int\frac{d^3q''}{(2\pi)^3}\tilde{\Pi}(\gamma_\alpha\tau_p,\gamma_\mu 1;\mathbf{q},\mathbf{q}'')\chi_V(q'')\Pi(\gamma^\mu 1,1;\mathbf{q}'',\mathbf{q}')\\&-\sum_{i=1}^{3}\int\frac{d^3q''}{(2\pi)^3}\tilde{\Pi}(\gamma_\alpha\tau_p,\gamma_\mu\tau_i;\mathbf{q},\mathbf{q}'')\chi_\rho(q'')\Pi(\gamma^\mu\tau_i,1;\mathbf{q}'',\mathbf{q}')\quad(\alpha,\beta=0,1,2,3).\end{aligned}$$

Here χ_s, χ_V, and χ_ρ are defined by

$$\chi_s(q,\omega)=\frac{g_s^2}{m_s^2-q_\lambda^2}\ ,$$

$$\chi_V(q,\omega)=\frac{g_V^2}{m_V^2-q_\lambda^2}\ , \tag{7}$$

$$\chi_\rho(q,\omega)=\frac{g_\rho^2}{4(m_\rho^2-q_\lambda^2)}\ ,$$

where g_s, g_V, and g_ρ are the coupling constants of the σ, ω, and ρ mesons, and m_s, m_V, and m_ρ are their masses. For these parameters we use the same values as in Ref. 5, determined in Ref. 2 from the saturation properties of nuclear matter and the rms charge radius of ^{40}Ca.

The isospin factors are easily evaluated. The propagator $\Pi(A,B)$ given in Eq. (3) can be rewritten in terms of the Green's matrix G:[6]

$$\Pi(A(\mathbf{x}),B(\mathbf{y});\omega)=\sum_{\mathrm{h}}\left[\bar{\Psi}_{\mathrm{h}}(\mathbf{x})\Gamma_A{}^{\dagger}\sum_{\mathrm{p}}\left[\frac{\Psi_{\mathrm{p}}(\mathbf{x})\bar{\Psi}_{\mathrm{p}}(\mathbf{y})}{E_{\mathrm{p}}-(E_{\mathrm{h}}+\omega)-i\epsilon}\right]\Gamma_B\Psi_{\mathrm{h}}(\mathbf{y})+\bar{\Psi}_{\mathrm{h}}(\mathbf{y})\Gamma_A\sum_{\mathrm{p}}\left[\frac{\Psi_{\mathrm{p}}(\mathbf{y})\bar{\Psi}_{\mathrm{p}}(\mathbf{x})}{E_{\mathrm{p}}-(E_{\mathrm{h}}-\omega)+i\epsilon}\right]\Gamma_B{}^{\dagger}\Psi_{\mathrm{h}}(\mathbf{x})\right]$$

$$=\sum_{\mathrm{h}}[\Psi_{\mathrm{h}}^{\dagger}(\mathbf{x})\gamma_0\Gamma_A{}^{\dagger}G(\mathbf{x},\mathbf{y};E_{\mathrm{h}}+\omega)\gamma_0\Gamma_B\Psi_{\mathrm{h}}(\mathbf{y})+(\Psi_{\mathrm{h}}^{\dagger}(\mathbf{x})\Gamma_B^{\dagger}\gamma_0G(\mathbf{x},\mathbf{y};E_{\mathrm{h}}-\omega)\Gamma_A^{\dagger}\gamma_0\Psi_{\mathrm{h}}(\mathbf{y}))^*] \tag{8}$$

[$\Psi_{\mathrm{p,h}}$ wave function of a nucleon particle or hole]. Using the decomposition[11]

$$G(\mathbf{x},\mathbf{y},E)=\sum_{\kappa,m}\frac{1}{xy}\begin{bmatrix} g_{11}^{\kappa}\mathcal{Y}_{\kappa m}(\Omega_x)\mathcal{Y}^*_{\kappa m}(\Omega_y) & -ig_{12}^{\kappa}\mathcal{Y}_{\kappa m}(\Omega_x)\mathcal{Y}^*_{-\kappa m}(\Omega_y)\\ ig_{21}^{\kappa}\mathcal{Y}_{-\kappa m}(\Omega_x)\mathcal{Y}^*_{\kappa m}(\Omega_y) & g_{22}^{\kappa}\mathcal{Y}_{-\kappa m}(\Omega_x)\mathcal{Y}^*_{-\kappa m}(\Omega_y)\end{bmatrix}\ , \tag{9}$$

where

$$\mathcal{Y}_{\kappa m}(\Omega)=\sum_{m'}Y_{l(\kappa)m'}(\Omega)\chi_{(1/2)m-m'}\langle l(\kappa),m',\tfrac{1}{2},m-m'\,|\,j(\kappa),m\rangle \tag{10}$$

with

$$\chi_{1/21/2}=\begin{bmatrix}1\\0\end{bmatrix},\quad \chi_{1/2-1/2}=\begin{bmatrix}0\\1\end{bmatrix},$$

$$j=|\kappa|-\tfrac{1}{2}\ ,$$

$$m=j_z\ ,$$

$$l=\begin{cases}\kappa; & \kappa>0\\ -\kappa-1; & \kappa<0\ ,\end{cases}$$

the full Green's matrix is reduced to the radial Green's matrix, which is a solution of the inhomogeneous Dirac equation

$$\begin{bmatrix}-M^*-V+E & \dfrac{d}{dx}-\dfrac{\kappa}{x}\\ \dfrac{d}{dx}+\dfrac{\kappa}{x} & -M^*+V-E\end{bmatrix}\begin{bmatrix}g_{11}^{\kappa} & g_{12}^{\kappa}\\ g_{21}^{\kappa} & g_{22}^{\kappa}\end{bmatrix}$$

$$=\delta(x-y)\begin{bmatrix}-1 & 0\\ 0 & 1\end{bmatrix} \tag{11}$$

with

$$V(\mathbf{x})=g_V V_0(\mathbf{x})+\tfrac{1}{2}g_\rho b_0(\mathbf{x})\tau_3+\tfrac{1}{2}(1+\tau_3)A_0(\mathbf{x}) \tag{12}$$

$$M^*(\mathbf{x})=M-g_s\phi_0(\mathbf{x})\ . \tag{13}$$

Here, $\phi_0(x)$, $V_0(x)$, and $b_0(x)$ are the expectation values of the fields of the σ, ω, and ρ mesons, and A_0 is the Coulomb field. Together with the nucleon wave functions, they are obtained from the solution of the mean-field equations of the $\sigma\omega\rho$ model for closed-shell nuclei as given in Ref. 2. The radial Green's matrix is calculated numerically as a proper combination of the regular and irregular solutions of the homogeneous part of Eq. (11).[11] Since $\tilde{\Pi}$ and Π are not very different, we solve the system Eq. (6) iteratively. With the notation

$$\begin{aligned}&\delta\Pi_{L,D}^{(\mathrm{n})}=\tilde{\Pi}_{L,D}^{(\mathrm{n})}-\Pi_{L,D}\ ,\\ &\Pi_{\mu,\nu}(\mathbf{q}_1,\mathbf{q}_2)=\Pi(\gamma_\mu\tau_{\mathrm{p}},\gamma_\nu\tau_{\mathrm{p}};\mathbf{q}_1,\mathbf{q}_2)\ ,\\ &\Pi_{s,\nu}(\mathbf{q}_1,\mathbf{q}_2)=\Pi(1\tau_{\mathrm{p}},\gamma_\nu\tau_{\mathrm{p}};\mathbf{q}_1,\mathbf{q}_2)\ ,\\ &\Pi_{\nu,s}(\mathbf{q}_1,\mathbf{q}_2)=\Pi(\gamma_\nu\tau_{\mathrm{p}},1\tau_{\mathrm{p}};\mathbf{q}_1,\mathbf{q}_2)\ ,\\ &\Pi_{s,s}(\mathbf{q}_1,\mathbf{q}_2)=\Pi(1\tau_{\mathrm{p}},1\tau_{\mathrm{p}};\mathbf{q}_1,\mathbf{q}_2)\ ,\end{aligned} \tag{14}$$

the first two iterations read

$$\delta\Pi^{(1)}_{L,D}(\mathbf{q},\mathbf{q}')=\int\frac{d^3q''}{(2\pi)^3}\chi_s(q'')\Pi_{0,s}(\mathbf{q},\mathbf{q}'')\Pi_{s,0}(\mathbf{q}'',\mathbf{q}')$$
$$-\int\frac{d^3q''}{(2\pi)^3}\chi_V(q'')\Pi^{\mu}_{0}(\mathbf{q},\mathbf{q}'')\Pi_{\mu,0}(\mathbf{q}'',\mathbf{q}')-\int\frac{d^3q''}{(2\pi)^3}\chi_\rho(q'')\Pi^{\mu}_{0}(\mathbf{q},\mathbf{q}'')\Pi_{\mu,0}(\mathbf{q}'',\mathbf{q}')\ , \tag{15}$$

$$\delta\Pi^{(2)}_{L,D}(\mathbf{q},\mathbf{q}')=\delta\Pi^{(1)}_{L,D}(\mathbf{q},\mathbf{q}')+2\int\frac{d^3q''}{(2\pi)^3}\int\frac{d^3q'''}{(2\pi)^3}[\,\chi_s(q'')\chi_s(q''')\Pi_{0,s}(\mathbf{q},\mathbf{q}''')\Pi_{s,s}(\mathbf{q}''',\mathbf{q}'')\Pi_{s,0}(\mathbf{q}'',\mathbf{q}')$$
$$-2\chi_s(q'')\chi_V(q''')\Pi_{0,\mu}(\mathbf{q},\mathbf{q}''')\Pi^{\mu}_{s}(\mathbf{q}''',\mathbf{q}'')\Pi_{s,0}(\mathbf{q}'',\mathbf{q}')$$
$$+\chi_V(q'')\chi_V(q''')\Pi_{0,\nu}(\mathbf{q},\mathbf{q}''')\Pi^{\nu,\mu}(\mathbf{q}''',\mathbf{q}'')\Pi_{\mu,0}(\mathbf{q}'',\mathbf{q}')$$
$$+\chi_\rho(q'')\chi_\rho(q''')\Pi_{0,\nu}(\mathbf{q},\mathbf{q}''')\Pi^{\nu,\mu}(\mathbf{q}''',\mathbf{q}'')\Pi_{\mu,0}(\mathbf{q}'',\mathbf{q}')]\ . \tag{16}$$

The further calculation proceeds as follows. The wave functions Ψ_h of the nucleons are, analogously to the Green's matrix, decomposed into angular and radial parts. The angular integrations in Eq. (2) can then be done analytically; the radial integrals are evaluated numerically. The results for $\Pi(\mathbf{q}_1,\mathbf{q}_2)$ are inserted in Eqs. (15) and (16). Again, the angular integrations are performed analytically; the radial integrations with respect to q'' and q''', numerically.

III. RESULTS

In Fig. 1 we show, for $\mathbf{q}'\|\mathbf{q}$, the imaginary part of the polarization propagator

$$\Pi(\gamma_0\tau_p,\gamma_0\tau_p;\mathbf{q},\mathbf{q}';\omega)=\Pi_{L,D}(q,q') \tag{17}$$

at fixed q and ω as a function of q' for different nuclei. The maximum approaches $q'=q$, and the function becomes narrower with the increasing size of the nucleus. This reflects the decrease of nonlocality in momentum space as translational invariance tends to be restored. Similar behavior is also observed in nonrelativistic calculations of the polarization propagator for finite nuclei.[8]

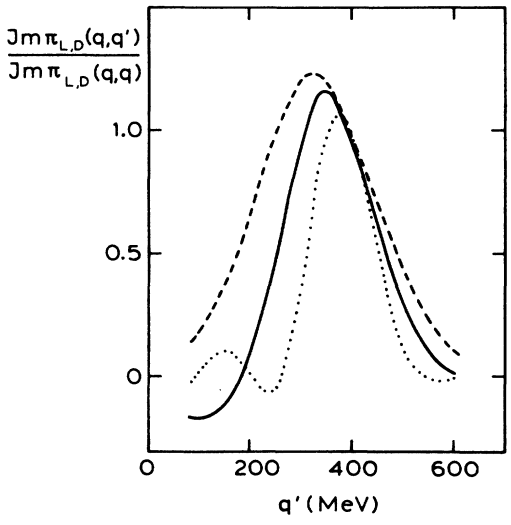

FIG. 1. Imaginary part of the polarization propagator $\Pi(\gamma_0,\gamma_0;\mathbf{q},\mathbf{q}';\omega)=\Pi_{L,D}(q,q')$ for $\mathbf{q}'\|\mathbf{q}$ and $q=400$ MeV, $\omega=50$ MeV as a function of q'. The dashed, solid, and dotted lines show this function for ^{12}C, ^{40}Ca, and ^{208}Pb, respectively, normalized by its value at $q'=q$.

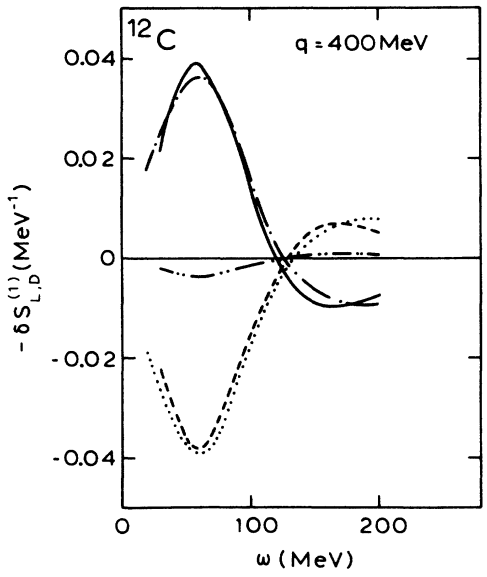

FIG. 2. RPA correction for the Dirac contribution to the longitudinal response function, in first order of the iterative solution, for ^{12}C at $q=400$ MeV. The solid (dot-dashed) line shows the contribution from the scalar σ meson, evaluated with the exact one-body density (in local-density approximation). The same is shown for the vector ω meson by the dashed (dotted) lines, and for the vector isovector ρ meson by the dashed-two dotted line (there the results from the exact calculation and from local-density approximation are indistinguishable on this scale).

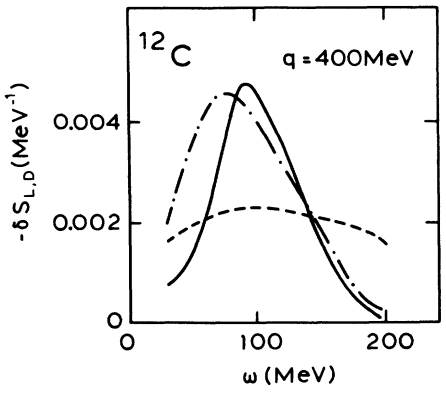

FIG. 3. Total RPA correction for the Dirac contribution to the longitudinal response function in first and second order of the iterative solution, for ^{12}C at $q=400$ MeV. The dashed (solid) line shows the result of the exact calculation in first (second) order; the dotted-dashed line the result for the exact matrix inversion in local-density approximation.

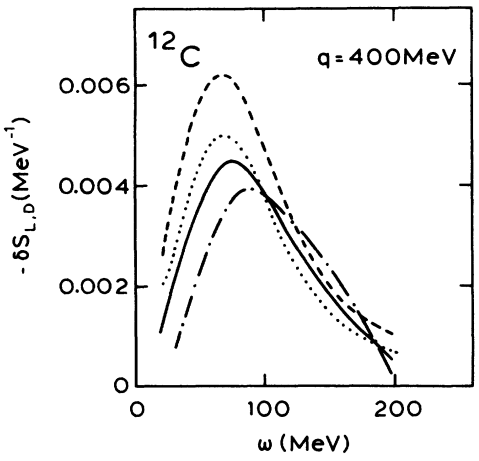

FIG. 5. Convergence of the iterative solution of the RPA equations in local-density approximation for ^{12}C, $q=400$ MeV. The dashed, dotted-dashed, and dotted lines show the result in first, second, and third order of the iteration. The solid line shows the result obtained from exact matrix inversion.

In Figs. 2–5 we compare the RPA correction to the Dirac part of the longitudinal response function

$$\delta S^{(n)}_{L,D}=\frac{1}{\pi}\mathrm{Im}\delta\tilde{\Pi}^{(n)}_{L,D} \tag{18}$$

as obtained from Eqs. (15) and (16), with that from the corresponding iterative solution of the RPA equation in nuclear matter, applied to nuclei in local-density approximation. The contributions from the σ, ω, and ρ mesons to $\delta S^{(1)}_{L,D}$ are shown separately in Fig. 2 for ^{12}C at $q=400$ MeV. It can be seen that the result of the exact calculation is very close to the result in local-density approximation. On the other hand, the total first correction is the sum of large and opposite contributions from the scalar and vector mesons, and, therefore, small relative differences in the individual contributions can result in large differences in the total correction. In Figs. 3 and 4 we show the total corrections in first and second iteration, for ^{12}C at $q=400$ MeV and $q=550$ MeV, together with local-density results. For $q=550$ MeV the iterative solution of the integral equations converges rapidly. For $q=400$ MeV the convergence is slower and it would be desirable to also calculate the third order $\delta S^{(3)}_{L,D}$. This is, however, not feasible with the exact one-body density because of the aforementioned delicate cancellation of the individual contributions which becomes more severe with increasing order of the iteration. Nevertheless, the RPA equations can be solved in higher orders of the iteration, and exactly in local-density approximation. These results are shown in Fig. 5 for ^{12}C, $q=400$ MeV, which gives first, second, third order, and the results from exact matrix inversion. The higher iterations and the exact results are quite close to each other. As shown in Fig. 4, the iteration series converges even faster for $q=550$ MeV. Thus, we have reason to believe that the second order of

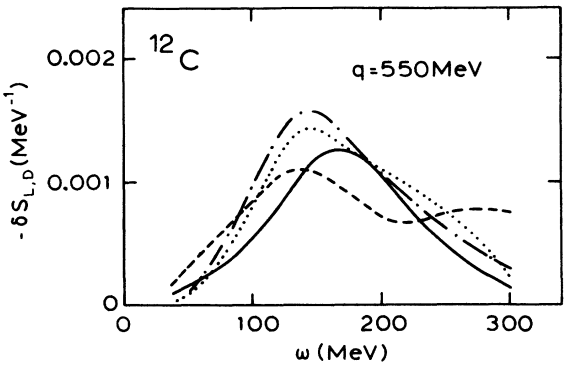

FIG. 4. Same as Fig. 3, but for ^{12}C at $q=550$ MeV. The additional dotted line shows the result of the second order of the iterative solution in local-density approximation.

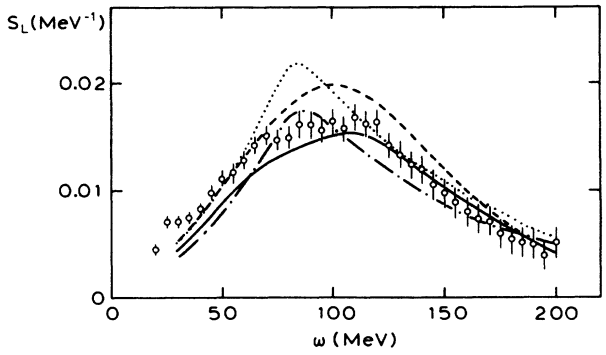

FIG. 6. Longitudinal response function for ^{12}C at $q=400$ MeV. The solid (dashed) line shows the result of the calculation using the exact one-body density with (without) the RPA correlations. The dotted-dashed (dotted) line shows the corresponding results in local-density approximation. The data are from Ref. 12.

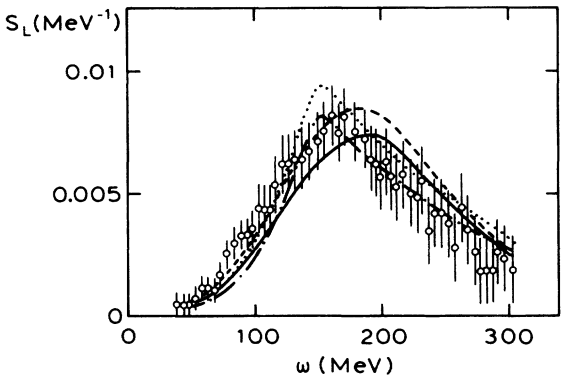

FIG. 7. Same as Fig. 6, but for ^{12}C at $q = 550$ MeV.

the iterative solution is sufficient for $q \geq 400$ MeV. We do not show results for $q = 300$ MeV, because there the convergence is quite slow and the second-order result may not be reliable. The same remarks also hold for ^{40}Ca.

We compare our results for ^{12}C, $q = 400$ MeV (Fig. 6) and $q = 550$ MeV (Fig. 7), and ^{40}Ca, $q = 410$ MeV (Fig. 8) and $q = 550$ MeV (Fig. 9), with the data.[12,13] First of all, we reproduce the results of Ref. 6 for the longitudinal response function in the Hartree approximation, including both the Dirac- and the anomalous current, and using the exact one-body density. Comparing with the corresponding Hartree result in local-density approximation,[5] the maximum is shifted towards a larger energy transfer, due to the inclusion of binding energy effects, and slightly broadened. We obtain our final result for the longitudinal response function in random-phase approximation by adding the RPA correction for the Dirac contribution of the longitudinal response to the Hartree result, both calculated with the exact one-body density. For ^{12}C the agreement with the data is, compared with the local-density approximation, slightly better for $q = 400$ MeV and slightly worse for $q = 550$ MeV, but quite good for both values of the momentum transfer. For ^{40}Ca we obtain good agreement at $q = 410$ MeV, but the response is

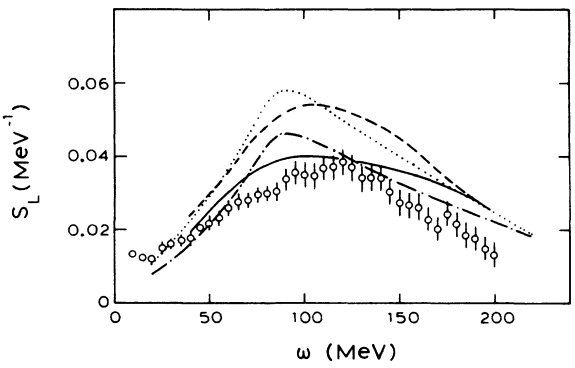

FIG. 8. Same as Fig. 6, but for ^{40}Ca at $q = 410$ MeV. The data are from Ref. 13.

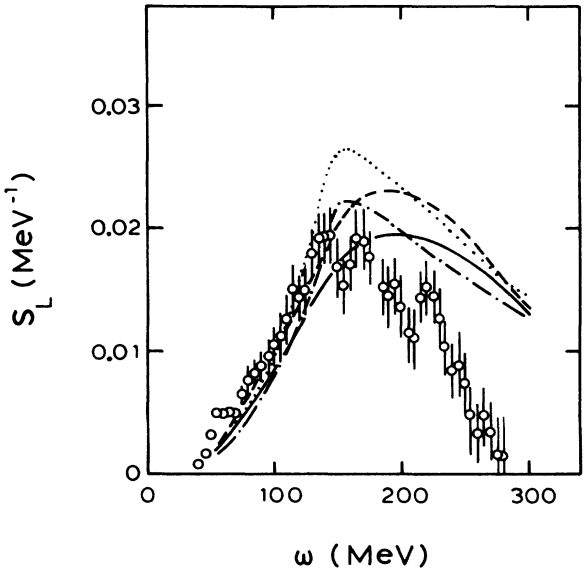

FIG. 9. Same as Fig. 6, but for ^{40}Ca at $q = 550$ MeV.

overestimated at large values of the energy transfer. This feature becomes more pronounced for $q = 550$ MeV, where the maximum of the response is shifted with respect to the data to a higher energy transfer.

IV. CONCLUSION

We have calculated the longitudinal response function for quasielastic electron scattering on ^{12}C and ^{40}Ca in the framework of the $\sigma\omega\rho$ model of quantum hadrodynamics. By using the wave functions and binding energies of the nucleons as obtained from mean-field theory of closed-shell nuclei, the structure of the nucleus is taken fully into account. Ground-state correlations are included in relativistic random-phase approximation which was developed for nuclear matter in Ref. 3 and is here generalized to finite nuclei. The integral equations of the relativistic random-phase approximation were solved iteratively for the dominant Dirac contribution to the longitudinal response.

Comparing with the results of a previous calculation[5] we find a shift in the position of the maximum due to the inclusion of binding energy effects. The response function evaluated with the exact one-body density is also slightly broader than that in local-density approximation. For ^{40}Ca the high energy shoulder is overestimated, especially at high momentum transfers. This may be due to a somewhat too small effective mass. We remind the reader in this connection of the fact that the Landau parameters of the self-consistent $\sigma\omega\rho$ model in its present form are not in agreement with observations,[14] leading, e.g., to a much too high compressibility.

The overall agreement with the data is, however, as good as in local-density approximations. Considering

also the results for the transverse response function as given in Refs. 6 and 5, we conclude that the $\sigma\omega\rho$ model of quantum hadrodynamics is capable of describing both the longitudinal and the transversal response for quasielastic electron scattering. Since this good agreement is obtained using the free nucleon form factors, we find no evidence for medium-modified form factors.

This work was supported by the Gesellschaft für Schwerionenforschung, Darmstadt.

[1]B. D. Serot and J. D. Walecka, *Advances in Nuclear Physics*, edited by J. W. Negele and E. Vogt (Plenum, New York, 1986), Vol. 16.
[2]C. J. Horowitz and B. D. Serot, Nucl. Phys. **A368**, 503 (1981).
[3]H. Kurasawa and T. Suzuki, Nucl. Phys. **A445**, 685 (1985).
[4]H. Kurasawa and T. Suzuki, Phys. Lett. B **173**, 377 (1986).
[5]K. Wehrberger and F. Beck, Phys. Rev. C **35**, 298 (1987); **35**, 2337 (1987).
[6]S. Nishizaki, H. Kurasawa, and T. Suzuki, Phys. Lett. B **171**, 1 (1986).
[7]G. F. Bertsch and S. F. Tsai, Phys. Rep. **18**, 125 (1975).
[8]W. M. Alberico *et al.*, Phys. Rev. C **34**, 977 (1986).
[9]W. M. Alberico, P. Gerski, M. Ericson, and A. Molinari, Nucl. Phys. **A462**, 269 (1987).
[10]A. L. Fetter and J. D. Walecka, *Quantum Theory of Many-Particle Systems* (McGraw-Hill, New York, 1971).
[11]P. J. Mohr, Ann. Phys. (N.Y.) **88**, 26 (1974).
[12]P. Barreau *et al.*, Nucl. Phys. **A402**, 515 (1983).
[13]Z. E. Meziani *et al.*, Phys. Rev. Lett. **52**, 2130 (1984).
[14]T. Matsui, Nucl. Phys. **A370**, 365 (1981).